Kyle Ann Huskin, Ivan Shevchuk

# Chapter 4: Multispectral Imaging (MSI) and Statistical Image Processing to Analyse Pigment Distribution and Diverse Material Features

**Abstract:** The multispectral imaging (MSI) data from the *tsakalis* was performed as a preliminary analysis to assist the work of other researchers involved in the project. Statistical processing of the spectral data identified potentially different pigments and thereby guided the measurements with X-ray fluorescence (XRF) and Raman spectroscopy. The infrared transmissive images showed the cards' paper structures for further analysis with microscopy and Fourier-transform infrared spectroscopy (FTIR). The high-resolution, accurate-colour images also served as a basis for palaeographic and art-historical study, as well as for computational pattern analysis work. The infrared reflectance images also revealed pre-drawings and symbols beneath the various colours, shedding light on the cards' production method. This chapter explains MSI as a method and discusses the findings related to pigment anomalies, underlying drawings and symbols, and paper structures.

## 1 Introduction

As a non-destructive and non-invasive method, multispectral imaging (MSI) is the go-to approach for recovering erased, palimpsested, or otherwise obscured text or features and has proven remarkably effective for this purpose. MSI can also be an effective tool to begin to study an object's materiality because it produces a diverse set of images with decent spectral resolution and excellent spatial resolution

<sup>1</sup> The 'Archimedes Palimpsest Project' of the early 2000s was the first MSI project to use digital photography and statistical processing methods, and its remarkable results established MSI as the go-to method for palimpsest text recovery (Netz and Noel 2007, 205–232; Easton and Noel 2010). More recently, MSI successfully recovered the undertext in Cambridge University Library's Codex Zacynthius (Houghton and Parker (eds) 2020; Easton et al. 2020). Useful for revealing more than text, MSI also uncovered spectacular drawings in Wolfenbüttel, Herzog August Bibliothek, Codex Guelf 125 Gud. lat. (Carmassi 2017). Similarly, MSI data from London, British Library, Cotton Nero A.x not only recovered damaged text and illustrations, but also revealed underdrawings and pigment anomalies (McGillivray and Duffy 2017).

that can easily facilitate different avenues of research. In the case of the tsakalis. MSI was performed with the latter goal in mind because they had no known illegible or obscured features.

The MSI results successfully guided and enabled the work of the other researchers and scholars on this project. For instance, statistical processing of the spectral data with Independent Component Analysis (ICA) produced a number of so-called 'pigment maps' that highlighted potential anomalies and thereby guided the initial, otherwise blind measurements with X-ray fluorescence (XRF) and Raman spectroscopy (see Chapter 9). The infrared transmissive images drew attention to differences among the cards' paper structures that were further explored with microscopy and Fourier-transform infrared spectroscopy (FTIR) (see Chapters 6 and 8, as well as the appendix). The high-resolution, accurate-colour images also fulfil all the typical needs of archival digitisation and thus served as a basis for palaeographic and art-historical study (see Chapters 1 and 3), as well as for computational pattern analysis work (see Chapter 5). Unexpectedly, the infrared reflectance images revealed letters beneath the various colours – a kind of paintby-numbers system – that was also of great interest to those analysing the pigments and the tsakalis' production methods.

## 2 Equipment and principles of MSI

All of the sixty-five tsakali cards were imaged in November 2021 by Ivan Shevchuk and Kyle Ann Huskin with the Centre for the Study of Manuscript Cultures' Mega-Vision EV<sup>™</sup> camera fitted with the 50-megapixel E7 sensor and a 120mm f/4.5 apochromatic lens.3 As per the usual setup, two equidistant tripods with three LED light panels each were stationed on either side of the camera. The panels illuminate in nineteen different wavelengths of light in the ultraviolet (UV), visible (VIS), and near infrared (NIR) parts of the electromagnetic spectrum, specifically from 365 to 1050 nanometres (nm). Two filter wheels mounted in front of the lens are used in combination with the UV wavelengths for the fluorescence part of the sequence. A customised LED light sheet is placed beneath the object to shine light at VIS and IR wavelengths through it. This setup allows us to capture up to fifty

<sup>2</sup> Janke et al. 2024 demonstrate that MSI can effectively reveal anomalous material features that merit further analysis with more specialised tools, such as XRF and FTIR.

<sup>3</sup> The system setup remains the same except that we have since upgraded to MegaVision's 150megapixel Q15 camera sensor (see <a href="https://mega-vision.com/products/ev-spectral-imaging-system/">https://mega-vision.com/products/ev-spectral-imaging-system/</a>, accessed on 22 July 2025).

grevscale images in four distinct imaging modalities: reflectance, fluorescence, raking, and transmissive.

The first two modalities - reflectance and fluorescence - are invaluable for text recovery and beneficial for ink and pigment classification. As the name suggests, the reflectance images capture light as it reflects off the surface of the object and into the camera lens. Specifically, the LEDs illuminate the object at 365, 385, 400, 420, 450, 470, 505, 530, 560, 590, 615, 630, 655, 700, 735, 780, 850, 940, and 1050 nm. These images are calibrated on a white Labsphere Spectralon® diffuse reflectance target, which reflects 99 per cent of light across the 350-1100 nm range detectable by the silicon camera sensor. Because humans can only see from roughly 400 to 700 nm, the reflectance images already reveal more information about the object than visible light alone. For instance, the three main ink classes (plant, iron-gall, and carbon inks) exhibit dramatically different optical properties in the NIR region.4 Likewise, the calibrated reflectance images – now reflectance data – enable a more comprehensive analysis of an artist's colour palette when researchers inspect the distinctive behaviour of some visually similar colours in the visible and invisible regions.<sup>5</sup> Finally, a highly accurate colour rendering is generated from the reflectance data by combining nine visible-light images. Using a Macbeth ColorChecker for colour calibration, these images are combined to produce a rendering in the LAB colour space – dubbed 'PSC' (Photoshoot Colour).

Fluorescence data is captured in up to twenty-two images when high-energy UV and blue light (365, 385, 400, and 450 nm) illuminates the object and excites its electrons into a higher energy level, causing them to decay and emit light at lower-energy wavelengths (i.e. in the VIS and NIR regions) depending on its features' material properties. The commonest manuscript substrates (e.g. parchment, paper, papyrus) readily fluoresce or 'glow' when illuminated with these wavelengths. The four fluorescence illuminations are combined with six filters (UV block (Schott GG400), UV pass (Hoya U360), orange (Wratten O22), red (Wratten R25), green (Wratten G58), and blue (Wratten B47)) that selectively prevent or permit certain wavelengths from reaching the camera sensor, improving the ability to distinguish amongst inks, stains, pigments, etc. Fluorescence data is invaluable for recovering faded and erased text written in plant and iron-gall inks, both of which penetrate deep into the substrate; even imperceptibly small amounts of remaining ink will quench the substrate's fluorescence, making it reappear against the

<sup>4</sup> See Mrusek, Fuchs and Oltrogge 1995, 72.

<sup>5</sup> McGillivray and Duffy 2017, 133-143, for example, use the 940 nm image to identify the presence of two red pigments (vermilion and what is presumed to be minium (red lead)) in the Gawain manuscript's illustrations.

glowing background. Fluorescence data can also be combined with infrared images to preliminarily identify some pigments if it can be compared to suitable reference target data.6

The final two imaging modalities – raking and transmissive – are more important for studying an object's materiality. Raking lights are placed at a 10-15° angle to the object and fired separately from the left and right panels at 450 and 940 nm, producing four images that enhance topographical features, such as erasures, scraping, cockling, etc. The final four images are captured when transmissive light is shone through the object at 500, 580, 735, and 940 nm to reveal substrate features, such as parchment thinning from ink corrosion or erasures, papyrus fibre structure, watermarks, chain and laid lines, and paper fibres.

# 3 Statistical image processing

After data capture, we use statistical image processing (or simply 'processing') to extract specific information from the greyscale images. An image cube with forty-two bands is created by digitally stacking the reflectance and fluorescence images. Every pixel has a numerical value from 0 to 4095 due to the camera sensor's 12-bit dynamic range. Because the images are registered, every pixel in every image refers to the same manuscript feature, and the pixels' changing numerical values correspond to the material's spectral changes across the wavelengths. This 'pixel dimensionality' allows us to use various statistical and algorithmic methods to enhance a given feature of the manuscript, typically the obscured text.

For both materials analysis and text recovery, the most consistently useful processing methods are Principal Component Analysis (PCA) and Independent Component Analysis (ICA).7 The PCA algorithm assumes a linear distribution of the dataset's statistics and uses an uncorrelated (orthogonal) transformation to reduce the dimensionality of a large dataset, such as an image cube, and reorder the information according to degree of difference, represented visually as contrast. The resulting PCA cube has a first band in which the most spectrally dissimi-

<sup>6</sup> Cosentino 2014, 4-9.

<sup>7</sup> For more on these methods' use in text recovery, see Easton and Kelbe 2014, 39-45. For more on ICA specifically, see Hyvärinen and Oja 2000. In this study, ICA was performed in ENVI Classic 5.7 from L3Harris Geospatial Solutions, Inc.

lar features (e.g. black and white pigments) are represented with the highest contrast, while the second band shows the second most dissimilar features (e.g. black or white pigments and another colour) with slightly less contrast, and so on. Unfortunately, manuscripts' highly heterogeneous features - e.g. stains, inks or pigments with variable thicknesses, flaking inks, overlapping pigments, irregularities in the substrate's texture or colouring, etc. – make it difficult for PCA to completely separate and accurately order the information.

We typically turn to ICA for features separation. ICA transforms the data based on higher-order statistics (e.g. kurtosis and negentropy) and reorders the data non-linearly according to degree of statistical independence. ICA is thus especially useful for separating mixed signals, extracting features, or identifying independent underlying patterns. It works well for manuscript analysis because the different inks and pigments on a page are essentially independent sources due to their unique spectral properties, and the MSI image cube contains the mixed signals of these independent sources. For this reason, ICA was chosen over PCA to compare the pigments used on the tsakalis in selected three-card datasets.8

#### 4 MSI results for the tsakalis

#### 4.1 Pigment distribution analysis

ICA was run on the nineteen calibrated reflectance images using a region of interest (ROI) on the middle tsakali in each of three selected datasets with the goal of 'mapping' pigments in each dataset,9 and spectral reflectance curves were also generated to supplement the ICA results. In most cases, the output ICA bands successfully isolated different coloured regions. In the case of red- and greencoloured areas, ICA indicated that different pigments may have been used for features that appear visually very similar. Combined with the spectral reflectance curves, the results conclusively demonstrated that two different green-coloured pigments (hereafter 'green' and 'teal-green') were used, but no solid conclusions could be drawn from the MSI data alone about the reds.

<sup>8</sup> Baronti et al. 1998, 1303-1309, show the potential for pigment mapping using PCA on MSI images. From what we know of ICA, it should work even better to separate pigments.

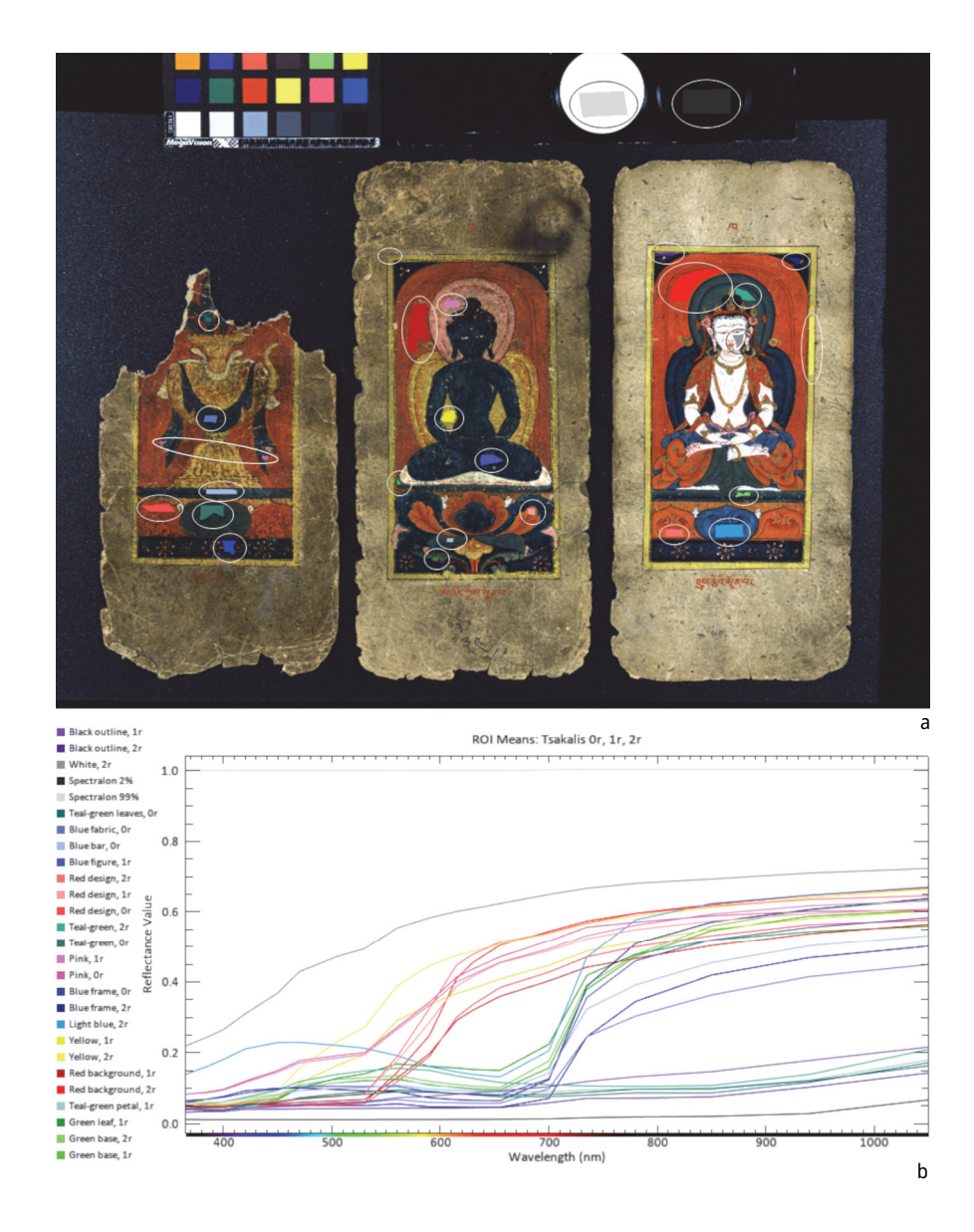
<sup>9</sup> All MSI data for the tsakalis are available in Shevchuk and Huskin 2024.

The first stage of analysis was comparing the ICA results to the colour image. We see in Figs 1a-h that several ICA bands clearly distinguish amongst the coloured regions in this dataset, including the blues, yellows, reds, and gold. However, we see in Fig. 1b that the algorithm did not separate but rather grouped the black outlines, borders, and hair with the teal-green areas in the cloud and leaves on Tsakali 0 recto, the lotus petal decoration (on which the Ye nyid kyis ston pa figure sits) on Tsakali 1 recto, and the mandorla and skirt on Tsakali 2 recto. Such grouping indicates that both colours have similar spectral responses. With Figs 1b and 1c, it becomes apparent that the green used for the leaves on Tsakali 1 recto, and for the deity figures' bases on Tsakali 1 recto and Tsakali 2 recto, should probably be distinguished from the teal-green used elsewhere - a sometimes-subtle colour distinction that may not be immediately apparent to the naked eye and something suggestive of different pigments. Moreover, there is noticeable confusion amongst the red areas in Figs 1e and 1f, raising the question of whether a different pigment could have been used for the background on Tsakali 2 recto, as well as whether different reds might have been used in the lower decorations across Tsakali 0 recto, Tsakali 1 recto, and Tsakali 2 recto.

The second stage of analysis was to create spectral reflectance curves for different coloured areas, focusing on those regions ICA identified as suspicious. We see in Figs 2a-b that the curves for each colour behave essentially the same regardless of where it was sampled. A striking exception occurs with the teal-green and green, which can appear visually quite similar: whereas the reflectance values for the green areas increase sharply at 655-700 nm, the teal-green areas' values remain low in the IR region. The 1050 nm images also confirm the colours' very different behaviours in wavelengths invisible to humans (see, for example, Figs 3a and 4b). These data strongly suggest that different pigments were used for the green and teal-green. For these pigments, then, MSI has been proven sufficient for preliminary pigment analysis, though it cannot identify the two pigments without supporting results from XRF and/or Raman spectroscopy.



Figs 1a-h: (a) PSC image of Tsakali 0 recto, Tsakali 1 recto, and Tsakali 2 recto; (b) ICA band 1, highlighting blacks and teal-greens; (c) ICA band 7, highlighting greens; (d) ICA band 10, highlighting gold; (e) ICA band 4, highlighting reds; (f) ICA band 9, highlighting reds and red-oranges; (g) ICA band 6, highlighting yellows; (h) ICA band 13, highlighting blues.



Figs 2a-b: (a) Selected ROIs shown as polygonal coloured areas, in circles, on the ENVI-generated RGB image of Tsakali 0 recto, Tsakali 1 recto, and Tsakali 2 recto; (b) spectral reflectance curves based on the mean ROI values.

Based on the ICA results in Figs 1e and 1f, we might also expect to see significant differences in the spectral reflectance curves for the two red background regions, as well as among the regions for the red decorations. The fact that all of the curves for their respective features follow similar trajectories, however, throws this assumption into doubt. These conflicting results highlight the limitations of reflectance MSI for pigment analysis. 10 All red pigments necessarily have similar reflectance curves in the VIS range, and MSI does not have the fine spectral resolution necessary to distinguish among them.11 For this reason, we cannot say if ICA is picking up some meaningful statistical difference that goes unnoticed in the spectral reflectance curves, such as different pigments or binders, or if ICA is amplifying some slight statistical variations that actually are not meaningful when it comes to pigment classification, such as variable thickness of pigment application or the relative cleanliness of the cards' surfaces. In this case, further analysis with XRF and/or Raman spectroscopy is needed to explain what, if anything, is causing these conflicting results in the MSI data.

Although the pigment distribution results were partially inconclusive, the MSI results were still immensely beneficial for highlighting suspicious features and guiding the initial XRF and Raman spectroscopy measurements so that these timeconsuming methods can be used most effectively (see Chapter 9).

#### 4.2 Pre-drawings revealed

Infrared wavelengths can penetrate thin layers of materials, such as a single layer of paper or most thinly applied pigments, more easily than visible light. For this reason, infrared reflectography (IRR), which typically operates in the 900-1700 nm range, is often used to visualise pre-drawings of paintings because those are usually done in with carbonaceous materials, such as graphite, which absorb light in the IR region.<sup>12</sup> The MSI data captured at 940 and 1050 nm did indeed reveal the tsakalis' pre-drawings (see Figs 3a-b). Unexpectedly, the images also revealed

<sup>10</sup> Cosentino 2014, 10, also struggles to differentiate red pigments with his UV-VIS-IR combinations and flowchart method. McGillivray and Duffy 2017, 133-143, could distinguish between vermilion and the suspected minium because an oxidised minium, like our teal-green and unlike vermilion, should remain dark throughout the IR region.

<sup>11</sup> Pigment mapping would probably be more successful with the higher spectral resolution of a hyperspectral imaging (HSI) system, which would capture over one hundred bands in the 365-1050 nm range. Bai, Messenger and Howell 2017, for example, found multiple kinds of visually similar red pigments on the Gough Map using Gram matrix analysis of HSI data.

<sup>12</sup> Delaney et al. 2016, 6-8.

characters under the main features of every tsakalis' illustration, and, upon closer examination, they seemed to refer consistently to the colours applied on top of them (see Figs 4a-c, as well as the more detailed explanation of the scheme in Chapter 3, 46-58).

The pre-drawings shed light on the tsakalis' production. They seem to suggest the following process: first, an artist drew with a carbon ink<sup>13</sup> the rectangular image frame, a line down the centre to aid symmetry, and outlines for the figures and most of the decorative elements in the same ink; next, the colours were laid down; and finally another layer of carbon-ink outlines were drawn or redrawn around the final image. 14 In Figs 3a-b showing fragments of Tsakali 1 recto, for instance, we can clearly see conflicting outlines in the IR images, most notably on the top curve of the Ye nyid kyis ston pa figure's nimbus and on his left leg and foot. Taking the nimbus (mandorla) as the clearer reference, it would appear that an artist laid down an initial, flatter outline in black ink; then the composition was altered intentionally or unintentionally when the pink and red layers were applied; and finally, the black outlines were redrawn according to the revised design.



Figs 3a-b: (a) Pre-drawings on Tsakali 1 recto revealed with the 1050 nm image, with PSC image for reference; (b) close-up of the pink nimbus region.

<sup>13</sup> The fact that the pre-drawings (and the letters, for that matter) appear dark in the IR and are absent in the XRF element maps indicates a carbonaceous composition.

<sup>14</sup> The full complexity of the production process is detailed in Chapter 3, 49–57.

Significantly, the IR images also uncovered letters that correspond to the colours in the illustration, suggesting that a kind of paint-by-numbers system was used in the production process. As shown in Figs 4a-c, this system is most clearly visible on Tsakali A recto because its intricate illustration utilises every colour from the whole tsakali set, but it appears consistently on every card. A system like this seems necessary only if the person designing the cards' initial layout, which includes these letters and the first layer of outlines, is different from the person applying the colours and final outlines. The IR images produced as part of the MSI analysis therefore provide valuable information for the art historians (see Chapter 3).

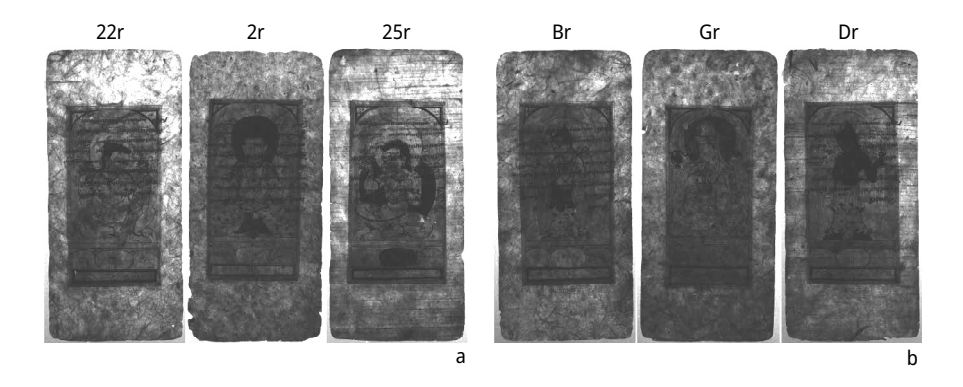


Figs 4a-c: (a) A catalogue of letters, taken from Tsakali A recto and Tsakali 0 recto, and their corresponding colours; (b) letters revealed on Tsakali A recto with the 1050 nm image, with the PSC image for reference; (c) letters denoting yellow revealed on Tsakali 0 recto with the 1050 nm image, with the PSC image for reference. Note: there is probably a symbol designating teal-green as well as green, but it may be invisible because the overlaid colour is equally dark at 1050 nm.

#### 4.3 Paper structure

The IR transmissive light images reveal what appeared to be three distinct types of paper: two types with inhomogeneous structures, randomly oriented fibres, and no visible laid lines, of which one type shows a lower and the other a higher

fibre density; and one with horizontal laid lines. 15 As shown in Figs 5a-b, the different paper types are present in both stylistic sets of tsakalis. Further analysis with microscopy and FTIR was, of course, necessary to understand crucial information about the paper, such as the fibre types used and the presence of additives, fillers, and sizing agents. Nevertheless, the MSI transmissive images offer some distinct advantages over the standard LED transmissive white light sheet for paper analysis. First, the paper structures are revealed better because of the better penetration properties of IR wavelengths than visible light. Second, the captured transmissive images are registered with the rest of the MSI data and allow for further visualisations by simply overlaying them with the reflectance data. Finally, the captured images allow anyone with the dataset, including the original researcher, to repeat the observations at any time. 16



Figs 5a-b: (a) Transmissive light images (940 nm) of three tsakalis from the first stylistic set showing, from left to right, the paper with lower-density fibre structure, with higher-density fibre structure, and with horizontal laid lines; (b) transmissive light images (940 nm) of three tsakalis from the second stylistic set showing the three types of paper in the same order.

<sup>15</sup> Later analysis (see Chapters 6 and 8) determined that there are two types of paper: a woven type with two subsets, one with a lower-density fibre structure and one with a higher-density structure, and a laid type with horizontal lines.

<sup>16</sup> Cf. McGillivray and Duffy 2017, 125.

## 5 Conclusion

MSI was successfully deployed as the first method of materials analysis on the tsakalis. The spectral data in the reflectance images, combined with statistical image processing, were able to distinguish conclusively between two sometimes very visually similar pigments – green and teal-green – and to raise questions about red pigments that guided further analysis with XRF and Raman spectroscopy. The IR images revealed not only pre-drawings but also letters indicative of a paint-by-numbers system hidden underneath the pigment layers, giving the art historians valuable new information. The transmissive images also assist paper analysis by providing a broad, repeatable overview of the entire tsakalis collection's substrates.